Electronic Supplementary Material (ESI) for Journal of Materials Chemistry A.

Supporting Information

3D Interconnected Porous Carbon Derived from Spontaneous Merging of the Nano-sized ZIF-8 Polyhedrons for High-Mass-Loading Supercapacitor Electrodes

Di Geng[a, 1], Su Zhang[b, 1], Yuting Jiang[a], Zimu Jiang[a], Mengjiao Shi[a], Jin Chang[a], Shichuan Liang[a], Mingyi Zhang[c], Jing Feng[a]*, Tong Wei[a, d]*, and Zhuangjun Fan[a, d]*

[a] Key Laboratory of Superlight Materials and Surface Technology, Ministry of Education; College of Material Science and Chemical Engineering, Harbin Engineering University, Harbin, 150001, P. R. China.

[b] State Key Laboratory of Chemistry and Utilization of Carbon Based Energy Resources; Key Laboratory of Energy Materials Chemistry, Ministry of Education; Key Laboratory of Advanced Functional Materials, Autonomous Region; Institute of Applied Chemistry, College of Chemistry, Xinjiang University, Urumqi, 830046, P. R. China.

[c] Key Laboratory for Photonic and Electronic Bandgap Materials, Ministry of Education, School of Physics and Electronic Engineering, Harbin Normal University, Harbin, 150025, P. R. China.

[d] State Key Laboratory of Heavy Oil Processing, School of Materials Science and Engineering, China University of Petroleum, Qingdao, 266580, P. R. China.

[1] These authors contributed equally to this work.

* Corresponding author.

E-mail address: fengjing@hrbeu.edu.cn (J. Feng) weitong666@163.com (T. Wei) fanzhj666@163.com (Z. Fan)

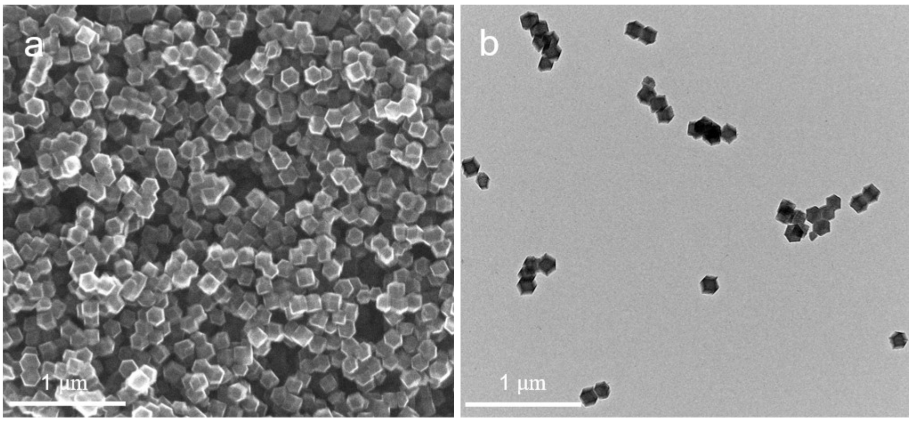

Figure S1. a) SEM and b) TEM images of LPC.

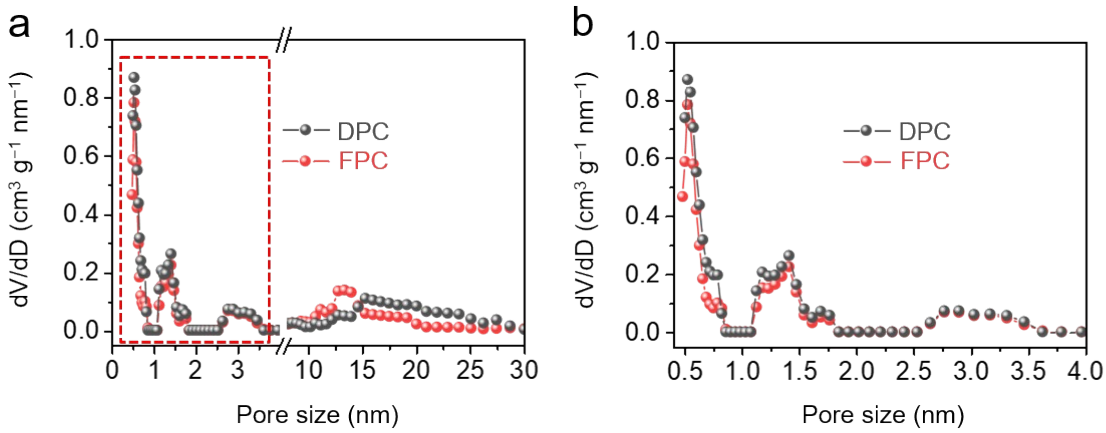

Figure S2. a) Pore size distribution and b) magnified micropore size distribution of DPC and FPC.

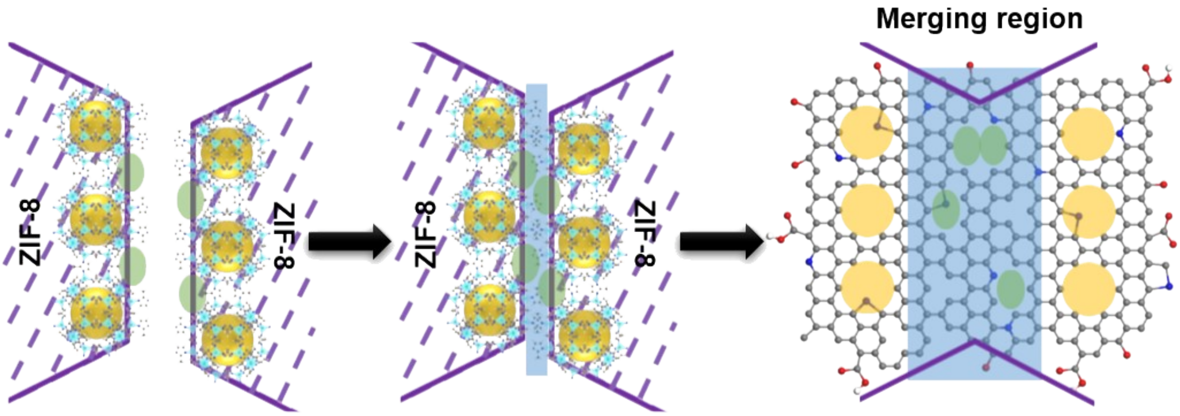

Figure S3. Schematic of the merging process.

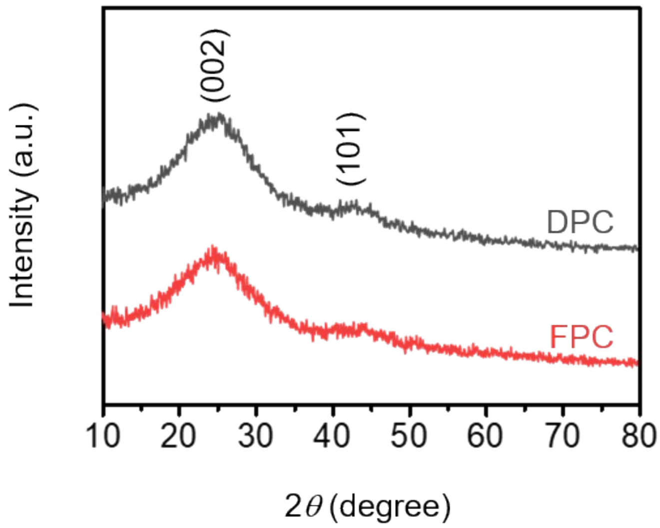

Figure S4. XRD patterns of DPC and FPC.

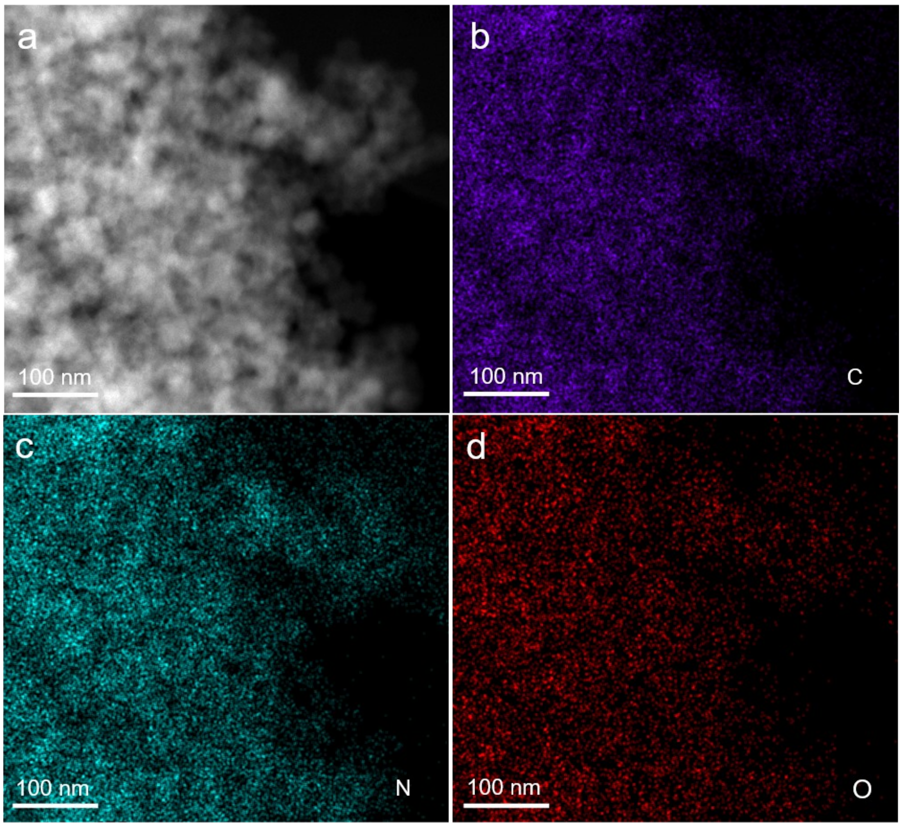

Figure S5. HRTEM image of a) DPC and the corresponding elemental mapping images of b) C, c) N, and d) O.

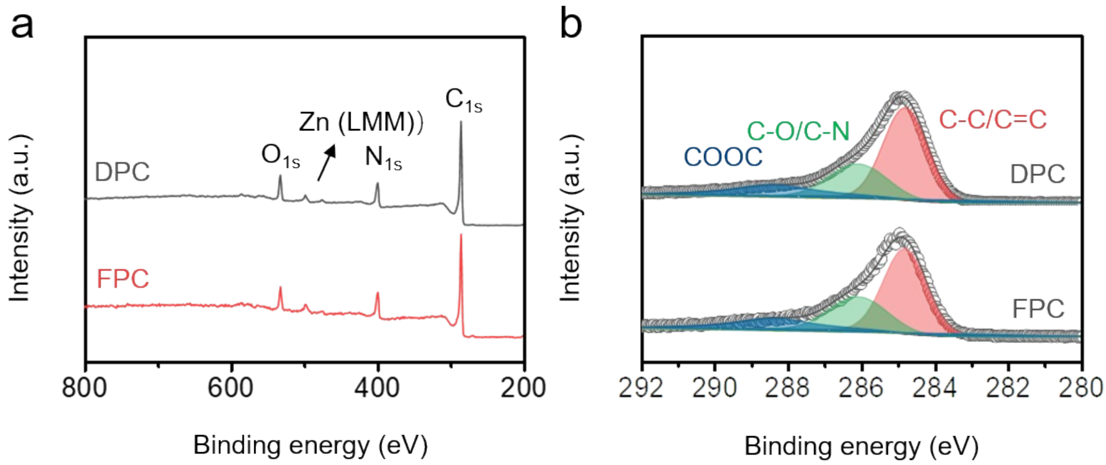

Figure S6. a) XPS survey spectra and b) C_{1s} spectra of DPC and FPC. The peak located at 495 eV indicates that some Zn species are remained in the internal of samples even after long-time acid washing and purification. However, due to the low content (DPC: 1.2 at.%, FPC: 2.4 at.%), we think that the residual Zn shows almost no influence on the electrochemical performance.

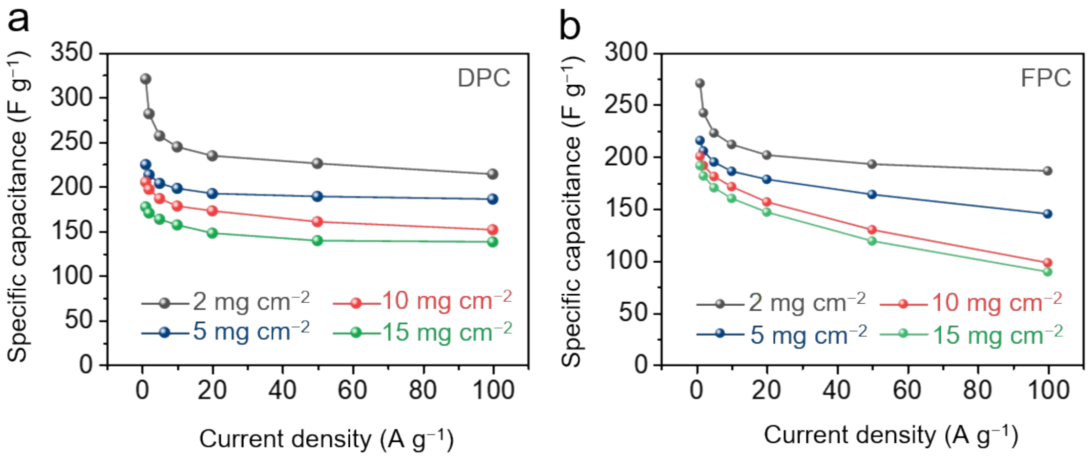

Figure S7. Specific capacitances of a) DPC and b) FPC at different current densities.

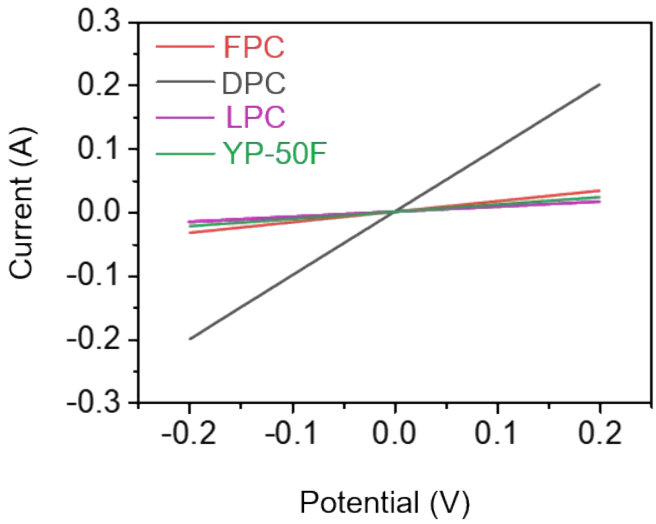

Figure S8. The I-V curves of FPC, DPC, LPC, and commercial activated carbon (YP-50F).

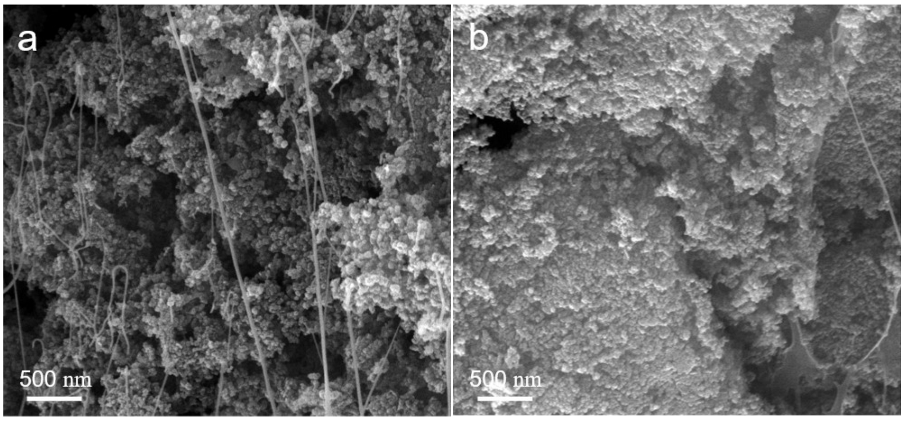

Figure S9. SEM images of the cross-section of a) FPC and b) DPC after compression under 10 MPa.

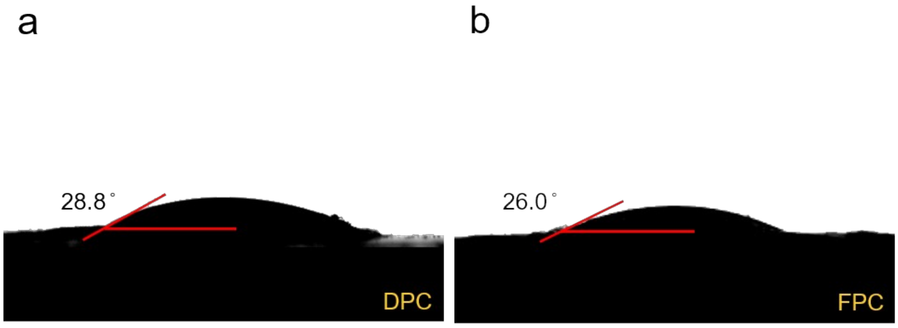

Figure S10. Contact angles of a) DPC and b) FPC toward 6 mol L^{-1} KOH aqueous electrolyte.

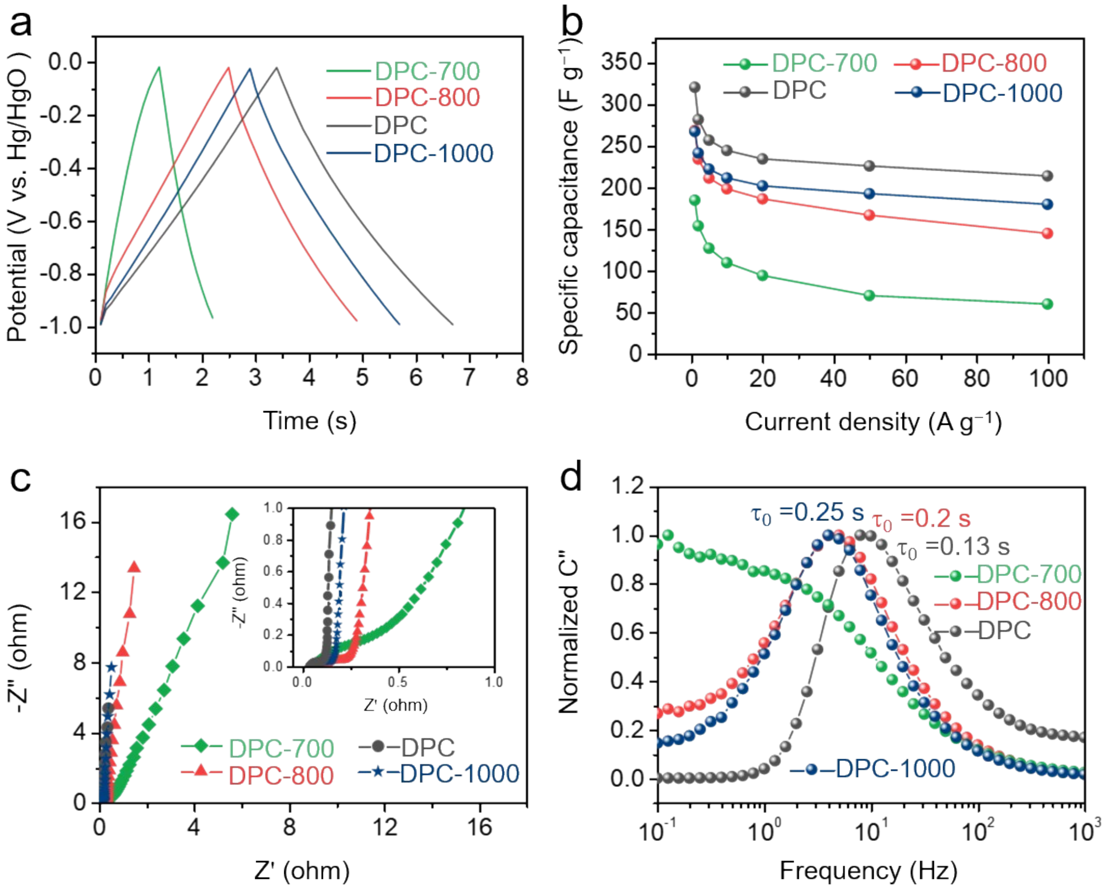

Figure S11. The electrochemical performance of DPC-700, DPC-800, DPC, and DPC-1000 samples measured by three-electrode system: a) GCD curves at 50 A g^{-1}, b) specific capacitances at different current densities, c) Nyquist plots, and d) normalized C''.

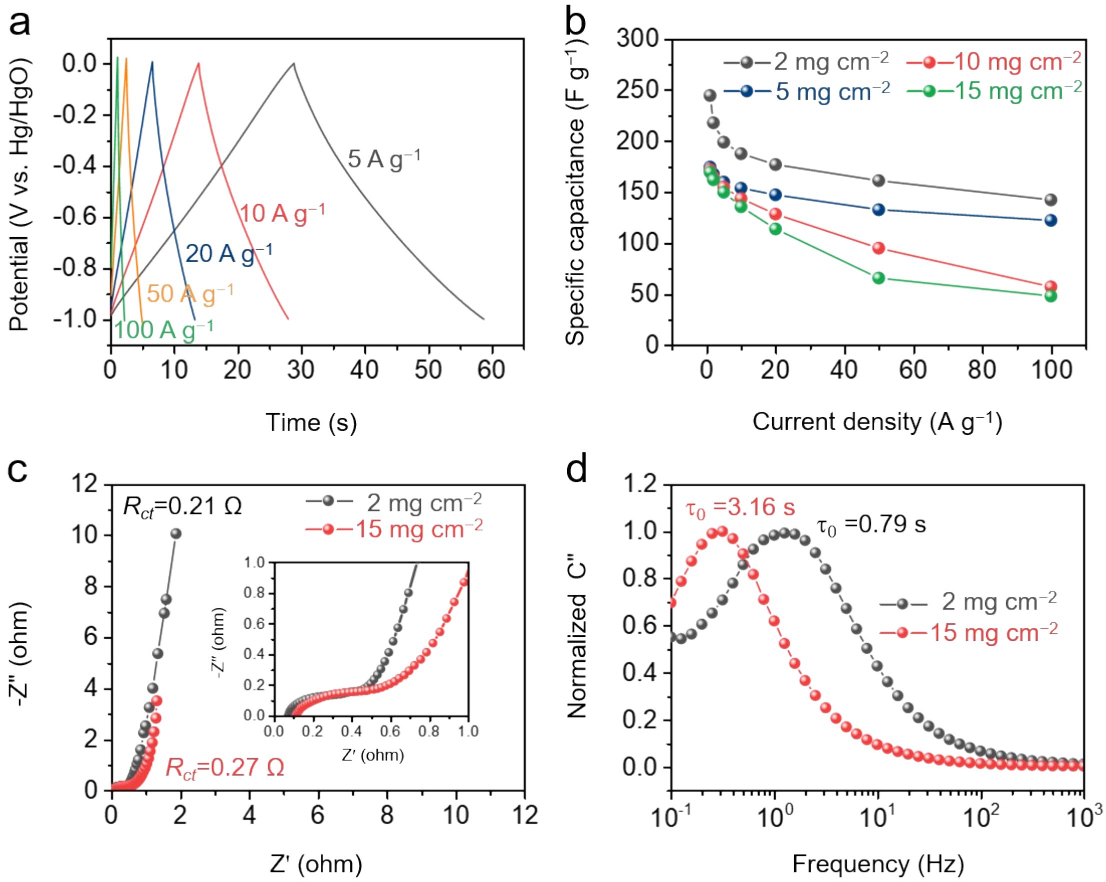

Figure S12. The electrochemical performance of LPC measured by three-electrode system: a) GCD curves at different current densities, b) specific capacitances at different current densities, c) Nyquist plots, and d) normalized C''.

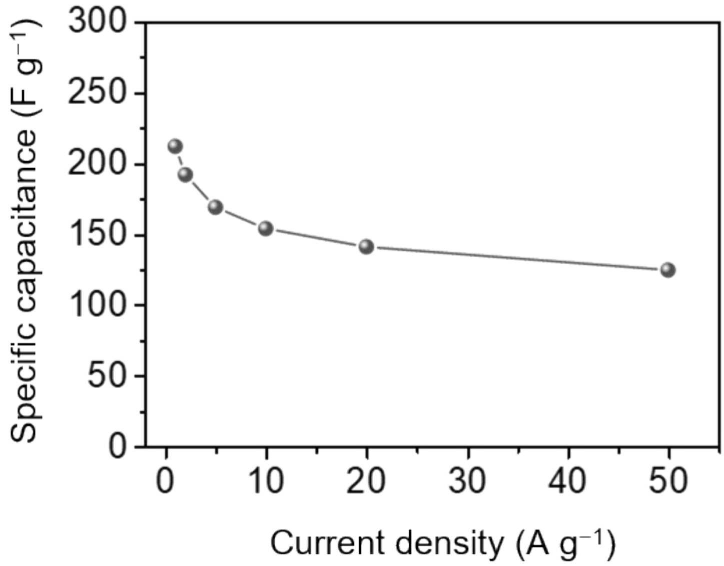

Figure S13. The specific capacitance of DPC based on two-electrode supercapacitor assembled using 1 mol L^{-1} Na_2SO_4 electrolyte.

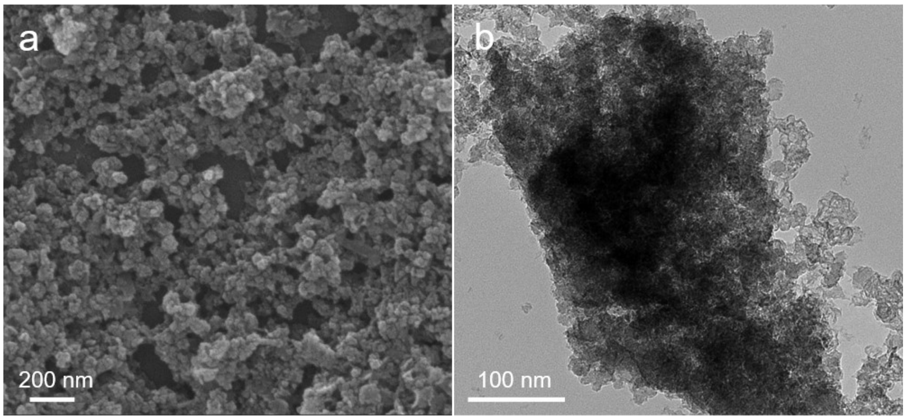

Figure S14. a) SEM and b) TEM images of the DPC after 10,000 cycles.

Table S1. Performance comparison of heteroatoms doped porous carbon-based materials.

Precursor	**Carbonization temperature (ºC)**	**Particle size (nm)**	**Doping elements**	**N (at%)**	**O (at%)**	**Electrolyte**	**Specific capacitance (F g^{-1} at X mVs^{-1})**	**Specific capacitance (F g^{-1} at Y A g^{-1})**	**Cycling stability**	**Energy density (Wh kg^{-1})**	**Power density (kW kg^{-1})**	**Ref.**
Zn-ZIF	800	-	N, O	12.9	6.2	6 mol L^{-1} KOH	-	221 (0.5) 184 (10)	10,000 cycles	22.8	63.1	**S1**
ZIF-8	950	200-300 nm	N	-	-	1 mol L^{-1} KOH	-	322(0.5) 215 (5)	10,000 cycles	-	-	**S2**
ZIF-8	800	200-400 nm	N, O	20.29	6.52	6 mol L^{-1} KOH	-	253.6 (1) 200.4 (50)	20,000 cycles (92.1%)	13.33	-	**S3**
ZIF-8	950	-	N	4.5	-	6 mol L^{-1} KOH	-	285.8 (0.1) 208 (2)	1000 cycles (97.8%)	-	-	**S4**
CNTs/ZIF-8	800	ca. 20 nm	N	4.1	-	6 mol L^{-1} KOH	-	324 (0.5) 152 (10)	1000 cycles (93.5 %)	-	-	**S5**

ZIF-8/CNT	900	ca. 300 nm	N, O	3.9	4.8	6 mol L^{-1} KOH	-	340 (2) 201 (50)	10,000 cycles (97.7%)	21.1	5	**S6**
ZIF-8/graphene	800	40~70 nm	N, O	18.6	3.9	6 mol L^{-1} KOH	-	225 (0.5) 181 (20)	10,000 cycles	6.5	15.126	**S7**
ZIF-8/graphene	800	500 nm/1 µm	N, O	13.5	10.8	6 mol L^{-1} KOH	-	298 (0.5)	-	8.7	12	**S8**
ZIF-8/melamine	800	300 nm	N, O	20.4	5.8	6 mol L^{-1} KOH	376.2 (10)	359.1 (1) 253.6 (20)	10,000 cycles (98.3%)	11.4	0.4985	**S9**
Porous organic silica	1000		O	-	>15	6 mol L^{-1} KOH	-	247 (1)	-	4.5	1.5	**S10**
Coal	800		O	13.65	0.92	6 mol L^{-1} KOH	-	259 (1) 198 (20)	10,000 cycles (94.2%)	9.6	0.25	**S11**
GO	-		O	-	>35	6 mol L^{-1} KOH	353 (2) 234 (500)	-	10,000 cycles	18	0.18	**S12**

GO	-		O	-	-	6 mol L^{-1} KOH	-	436 (0.5) 261 (50)	10,000 cycles (94%)	-	-	**S13**
Alfalal flower	700		O	-	13.5	6 mol L^{-1} KOH		350.1 (0.5) 297 (50)	-	23.2-28	10.3-0.1	**S14**
EDTA-3K	700		N, O	2.12	8.11	6 mol L^{-1} KOH	216.2 (5) 182.6 (100)	213.8 (1) 157.6 (20)	10,000 cycles (73.7%)	-	-	**S15**
Pomelo peel	700		N, O	5.2	5.5	6 mol L^{-1} KOH	-	180 (0.5) 136 (10)	5000 cycles (99%)	-	-	**S16**
Knoevenagel copolymer	700		N, O	3.5	9.61	6 mol L^{-1} KOH	-	330 (1) 221 (20)	-	24.9	0.18	**S17**
Organics	800		N, O	4.36	9.17	6 mol L^{-1} KOH	-	221 (0.5) 177 (8)	-	8.3	0.25	**S18**
ZIF-8	900	ca. 76 nm	N. O	14.2	8.1	6 mol L^{-1} KOH		320.7 (1) 213.9 (100)	10,000 cycles (100%)	7.6-20.6	34.3-0.5	**This work**

YP-50F	-	-	-	-	-	6 mol L^{-1} KOH	180.3 (1) 132.2 (100)	-	-	-	**This work**

Reference

[S1] J. Wang, J. Tang, B. Ding, Z. Chang, X. Hao, T. Takei, N. Kobayashi, Y. Bando, X. Zhang and Y. Yamauchi, *Small*, 2018, **14**, 1704461.

[S2] W. Bao, A. K. Mondal, J. Xu, C. Wang, D. Su and G. Wang, *J. Power Sources*, 2016, **325**, 286-291.

[S3] Z. Li, H. Mi, L. Liu, Z. Bai, J. Zhang, Q. Zhang and J. Qiu, *Carbon*, 2018, **136**, 176-186.

[S4] S. Zhong, C. Zhan and D. Cao, *Carbon*, 2015, **85**, 51-59.

[S5] L. Wan, E. Shamsaei, C. D. Easton, D. Yu, Y. Liang, X. Chen, Z. Abbasi, A. Akbari, X. Zhang and H. Wang, *Carbon*, 2017, **121**, 330-336.

[S6] Y. Liu, G. Li, Z. Chen and X. Peng, *J. Mater. Chem. A*, 2017, **5**, 9775-9784.

[S7] L. Wang, C. Wang, H. Wang, X. Jiao, Y. Ouyang, X. Xia, W. Lei and Q. Hao, *Electrochim. Acta*, 2018, **289**, 494-502.

[S8] L. Xin, Q. Liu, J. Liu, R. Chen, R. Li, Z. Li and J. Wang, *Electrochim. Acta*, 2017, **248**, 215-224.

[S9] C. Cai, Y. Zou, C. Xiang, H. Chu, S. Qiu, Q. Sui, F. Xu, L. Sun and A. Shah, *Appl. Surf. Sci.*, 2018, **440**, 47-54.

[S10] L. Zhang, X. Shen, K. Ai, X. Cui, H. Wang and W. Zheng, *ACS Appl. Energy Mater.*, 2019, **2**, 7009-7018.

[S11] D. Dong, Y. Zhang, Y. Xiao, T. Wang, J. Wang and W.-p. Pan, *Appl. Surf. Sci.*, 2020, **529**, 147074.

[S12] L. Jiang, L. Sheng, C. Long, T. Wei and Z. Fan, *Adv. Energy Mater.*, 2015, **5**, 1500771.

[S13] Z. Liu, L. Jiang, L. Sheng, Q. Zhou, T. Wei, B. Zhang and Z. Fan, *Adv. Funct. Mater.*, 2018, **28**, 1705258.

[S14] J. Yan, L. Miao, H. Duan, D. Zhu, Y. Lv, W. Xiong, L. Li, L. Gan and M. Liu, *Electrochim. Acta*, 2020, **358**, 136899.

[S15] J. Dai, L. Wang, A. Xie, J. He and Y. Yan, *ACS Sustainable Chem. Eng.*, 2020, **8**, 739-748.

[S16] J. Li, F. Luo, T. Lin, J. Yang, S. Yang, D. He, D. Xiao and W. Liu, *Chem. Phys. Lett.*, 2020, **753**, 137597.

[S17] X. Qian, L. Miao, J. Jiang, G. Ping, W. Xiong, Y. Lv, Y. Liu, L. Gan, D. Zhu and M. Liu, *Chem. Eng. J.*, 2020, **388**, 124208.

[S18] S. Meng, Z. Mo, Z. Li, R. Guo and N. Liu, *Mater. Chem. Phys.*, 2020, **246**, 122830.